Quantifying SO$_2$ oxidation pathways to atmospheric sulfate by using stable sulfur and oxygen isotopes: laboratory simulation and field observation

Ziyan Guo[a], Keding Lu[a]*, Pengxiang Qiu[b], Mingyi Xu[b], Zhaobing Guo[b]*

[a] State Key Joint Laboratory of Environmental Simulation and Pollution Control, State Environmental Protection Key Laboratory of Atmospheric Ozone Pollution Control, College of Environmental Sciences and Engineering, Peking University, Beijing, China.

[b] Jiangsu Key Laboratory of Atmospheric Environment Monitoring and Pollution Control (AEMPC), Collaborative Innovation Center of Atmospheric Environment and Equipment Technology (CIC-AEET), School of Environmental Science and Engineering, Nanjing University of Information Science and Technology, Nanjing 210044, China

Correspondence to: k.lu@pku.edu.cn *(Keding Lu),* guocumt@nuist.edu.cn *(Zhaobing Guo)*

Abstract. The formation of secondary sulfate in the atmosphere remains controversial, and it is urgent to seek for a new method to quantify different sulfate formation pathways. Thus, SO_2 and $PM_{2.5}$ samples were collected from 4 to 22 Dec. 2019 in Nanjing region. Sulfur and oxygen isotopic compositions were synchronously measured to study the contribution of SO_2 homogeneous and heterogeneous oxidation to sulfate. Meanwhile, the correlation of $\delta^{18}O$ values between H_2O and sulfate from SO_2 oxidation by H_2O_2 and Fe^{3+}/O_2 were simulatively investigated in the laboratory. Based on isotope mass equilibrium equations, the ratios of different SO_2 oxidation pathways were quantified. The results showed that secondary sulfate constituted higher than 80% of total sulfate in $PM_{2.5}$ during the sampling period. Laboratory simulation experiments indicated that $\delta^{18}O$ value of sulfate was linearly dependent on $\delta^{18}O$ value of water, and the slopes of linear curves for SO_2 oxidation by H_2O_2 and Fe^{3+}/O_2 were 0.43 and 0.65, respectively. The secondary sulfate in $PM_{2.5}$ was mainly ascribed to SO_2 homogeneous oxidation by OH radicals and heterogeneous oxidation by H_2O_2 and Fe^{3+}/O_2. SO_2 heterogeneous oxidation was generally dominant during sulfate formation, and SO_2 oxidation by H_2O_2 predominated in SO_2 heterogeneous oxidation reactions with an average ratio around 54.6%. This study provided an insight into precisely evaluating sulfate formation by combining stable sulfur and oxygen isotopes.

1 Introduction

Sulfate is one of the prevalent components of $PM_{2.5}$ (Brüggemann et al., 2021; Huang et al., 2014; Yang et al., 2023). Sulfate makes up approximately 25% of $PM_{2.5}$ mass in Shanghai, 23% in Guangzhou and 10-33% in Beijing (Xue et al., 2016). The rapid sulfate formation is a crucial factor determining the explosive growth of fine particles and the frequent occurrence of severe haze events in China (Lin et al., 2022; Liu et al., 2020; Meng et al., 2023; Wang et al., 2021). Sulfate plays an important role in the chemical and physical processes in the troposphere and lower stratosphere, which significantly affects global climate change by scattering solar radiation and acting as cloud condensation nuclei (Gao et al., 2022; Ramanathan et al., 2001). Meanwhile, sulfate exerts a significant influence on air quality and public health (Abbatt et al., 2006).

In the past decades, numerous attempts have been made to evaluate SO_2 oxidation pathways involving in homogeneous and heterogeneous reactions. Traditionally, sulfate formation mechanisms mainly include SO_2 homogeneous oxidation by OH radicals and heterogeneous oxidation by H_2O_2, O_3 and O_2 catalyzed by transition metal ions (TMIs) in cloud/fog water droplets. The relative importance of different sulfate formation pathways is strongly dependent on oxidant concentrations, occurrence of fog/cloud events and pH of aqueous phase (Kuang et al., 2022; Oh et al., 2023). Generally, SO_2 homogeneous oxidation by OH radicals and heterogeneous oxidation by H_2O_2 are considered the most important pathways for sulfate production on the global scale (Seinfeld and Pandis, 1998). The photochemical reactivity during the winter in Beijing has been found to be relatively high, which favors the formation of reactive species such as OH radicals and H_2O_2, thereby facilitating SO_2 oxidation (Zhang et al., 2020). Xue et al. (2014) suggested that SO_2 oxidation by O_3 and H_2O_2 in aqueous phase contributed to the majority of total sulfate production. Liu et al. (2020) proposed that S(IV) oxidation by H_2O_2 in aerosol water could be an important pathway considering the ionic strength effect. He et al. (2018) found that the contribution of SO_2 oxidation by H_2O_2 could reach 88% during Beijing haze period. Ye et al. (2018) observed that SO_2 oxidation rate by H_2O_2 was 2-5 times faster than the summed rate of the other three oxidation pathways. As a result, actual contribution of SO_2 oxidation by H_2O_2 during the winter might be underestimated in the previous studies.

In addition, the presence of NO_2 is obviously favorable for SO_2 oxidation under the conditions of high relative humidity (RH) and NH_3. NH_3 can promote the hydrolysis of NO_2 dimers to HONO and

70 result in more sulfate formation on particle surface in humid conditions. However, this conclusion was

71 doubted by Liu et al. (2017) who believed that the reaction on actual fine particles with pH at 4.2 was

72 too slow to account for sulfate formation. Li et al. (2020) deemed that SO_2 oxidation by NO_2 might not

73 be a major oxidation pathway in China. Furthermore, GEOS-Chem modeling study suggested that NO_2

74 oxidation contributed less than 2% of total sulfate production. It is found that TMI pathway was very

75 important in highly polluted regions, and the contribution of metal-catalyzed SO_2 oxidation to sulfate

76 was as high as 49±10% in haze. Wang et al. (2021) also argued that SO_2 oxidation via TMI on aerosol

77 surface could be the dominant sulfate formation pathway. They found that manganese-catalyzed

78 oxidation of SO_2 contributed 69.2±5.0% in sulfate production. Overall, the mechanisms for sulfate

79 rapid growth remain unclear and controversial. Therefore, sulfate formation pathways need to be

80 further explored, and it is urgent to develop a new method to quantify different sulfate formation

81 processes.

82   Generally, sulfur isotopes allow for investigating SO_2 oxidation processes in the atmosphere because

83 of distinctive isotope fractionation associated with different oxidation reactions (Harris et al., 2013).

84 Harris et al. (2012) presented the respective sulfur isotope fractionation factors of SO_2 oxidation by OH

85 radicals, O_3/H_2O_2 and iron catalysis. Besides, the observed sulfur isotope fractionation of SO_2 oxidation

86 by H_2O_2 and O_3 appeared to be no significant difference. Therefore, the results were particularly useful

87 to determine the importance of transition metal-catalyzed oxidation pathway compared to other

88 oxidation pathways. However, other main SO_2 oxidation pathways could not be distinguished only

89 based on stable sulfur isotope determination.

90   Oxygen isotope ratio ($\delta^{18}O$) can be used to deduce sulfate formation processes due to those SO_2

91 oxidation pathways affect oxygen isotope of product sulfate differently. Especially, mass-independent

92 fractionation signals of oxygen isotopes (nonzero $\Delta^{17}O$, where $\Delta^{17}O=\delta^{18}O-0.52\times\delta^{17}O$) in sulfate are

93 usually adopted to investigate the contribution of different SO_2 oxidation pathways. This method can

94 identify the contribution of SO_2+O_3 pathway when high $\Delta^{17}O$ value (>3‰) is measured in sulfate.

95 However, there is presence of obvious uncertainty when interpreting the sulfate with low $\Delta^{17}O$ value

96 (<1‰). Unfortunately, most sulfate samples in the atmosphere present $\Delta^{17}O<1‰$, suggesting a limited

97 contribution of SO_2+O_3 pathway during sulfate formation. It is noteworthy that the contribution of

98 $SO_2+H_2O_2$ and TMI pathway is unclear if solely using $\Delta^{17}O$ (Li et al., 2020). Holt and Kumar (1984)

99 found oxygen isotope was a valuable and complementary method to determine probable mechanisms of

100 SO_2 oxidation to sulfate in the atmosphere. This provides us an insight into precisely evaluating sulfate

101 formation pathways by combining oxygen and sulfur isotopes.

102 In this contribution, $PM_{2.5}$ and SO_2 were sampled from 4 to 22 Dec. 2019 in Nanjing. Sulfur and

103 oxygen isotopic compositions were measured to study the contribution of SO_2 homogeneous and

104 heterogeneous oxidation during sulfate formation. In addition, the linear relationships of $\delta^{18}O$ values

105 between H_2O and sulfate from SO_2 oxidation by H_2O_2 and Fe^{3+}/O_2 were synchronously investigated in

106 the laboratory. Based on sulfur and oxygen isotopes mass equilibrium equations, the ratios of different

107 SO_2 oxidation pathways during the sampling period were calculated. The study aims to seek for a novel

108 method to quantify different SO_2 oxidation processes with sulfur and oxygen isotopes.

109 **2 Materials and methods**

110 2.1 Sampling location

111 $PM_{2.5}$ and SO_2 in the atmosphere were sampled from 4 to 22 Dec. 2019 in Nanjing, China. The

112 sampling site was located at the roof of the library in Nanjing University of Information Science &

113 Technology (NUIST, 32.1° N, 118.5° E), which is depicted in Fig. 1. The sampling location is at the

114 side of Ningliu Road and closely next to Nanjing chemical industry park. There is presence of some

115 large-scale chemical enterprises such as Nanjing steel plant, Nanjing thermal power plants and Nanjing

116 petrochemical company, which inevitably release lots of SO_2 and iron metal into the atmosphere.
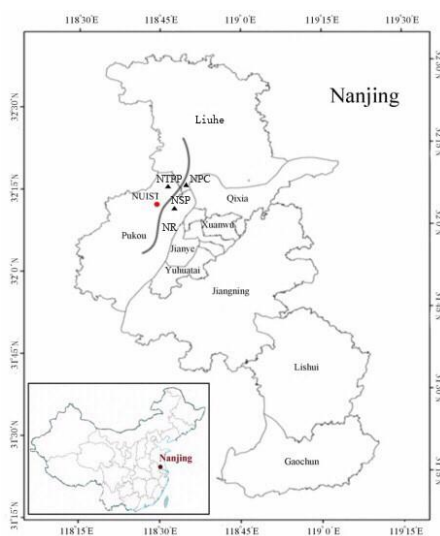
117

118 Fig.1. Sampling site of NUIST in Nanjing, China. NSP: Nanjing steel plants; NTPP: Nanjing

119 thermal power plants; NPC: Nanjing petrochemical company; NR: Ningliu Road.

120   2.2 $PM_{2.5}$ and SO_2 samples collection

121      $PM_{2.5}$ and SO_2 were sampled by using a modified JCH-1000 sampler (Juchuang Co., Qingdao) with

122   a flow rate of 1.05 $m^3 min^{-1}$ from 8 am to 8 pm from 4 to 22 Dec. 2019. $PM_{2.5}$ and SO_2 were collected

123   with quartz filter (203×254 mm, Munktell, Sweden) and glass fiber filter (203×254 mm, Tisch

124   Environment INC, USA), respectively. The filters were incinerated in a muffle furnace at 450 °C for 2h

125   and then preserved in the desiccators at room temperature. The glass fiber filters were firstly soaked in

126   2% K_2CO_3 and 2% glycerol solution for 2h and dried in DGG-9070A electric oven. SO_2 can be

127   changed into sulfite immediately during the sampling.

128   2.3 Extractions of water-soluble sulfate

129      $PM_{2.5}$ sample filters were shredded and soaked in 400 mL of Milli-Q (18 MΩ) water for extractions

130   of water-soluble sulfate. Filters were then isolated from solutions by centrifugation and sulfate was

131   precipitated as $BaSO_4$ by adding 1 mol L^{-1} $BaCl_2$. After the filtration with 0.22 μm acetate membrane,

132    $BaSO_4$ precipitate was rinsed with Milli-Q water to remove Cl^-. Finally, $BaSO_4$ powers were calcined

133   at 800 °C for 2h to obtain high purity $BaSO_4$. In addition, a small amount of H_2O_2 solution was added

134   to oxidize sulfite to sulfate.

135   2.4 Laboratory simulation of SO_2 oxidation by H_2O_2 and Fe^{3+}/O_2

136   For SO_2 oxidation by H_2O_2, 30 mL min^{-1} Ar was firstly introduced into three kinds of different water

137   about 30 min to drive out air. Sulfate was produced by adding 10 mL H_2O_2 dilute solution (0.1 mL 30%

138   H_2O_2 in 50 mL water) to SO_2 in the reaction chamber at 10 °C. H_2O_2 solution was agitated vigorously

139   for 1min before admission of air. For SO_2 oxidation by Fe^{3+}/O_2, 2 mL min^{-1} SO_2 and 2 mL min^{-1} O_2

140   were simultaneously put into Fe^{3+} dilute solution at 10 °C. Then, 10 mL 1 mL min^{-1} $BaCl_2$ was added to

141   prepare $BaSO_4$. Oxygen isotopic compositions of product sulfate and three kinds of water were

142   measured to study their linear relationships.

143   2.5 Sulfur and oxygen isotope determination

144   Sulfur isotopic compositions in sulfate were analyzed using Elemental analyzer (EA, Flash 2000,

145   Thermo) and isotope mass spectrometer (IRMS, Delta V Plus, Finningan). High-purity $BaSO_4$ was

146   converted into SO_2 in EA in the presence of Cu_2O. SO_2 from EA was ionized and $\delta^{34}S$ value was

147   measured using IRMS. For the determination of $\delta^{18}O$, $BaSO_4$ pyrolysis was conducted in graphite

148   furnace at 1450 ℃, and $\delta^{18}O$ value was obtained in CO produced from the pyrolysis at continuous-flow

149   mode. The results of $\delta^{34}S$ and $\delta^{18}O$ were with respect to international standard V-CDT and V-SMOW,

150   and the accuracy were better than ±0.2‰ and ±0.3‰, respectively.

151   **3 Results and discussion**

152   3.1 Concentrations of $PM_{2.5}$, sulfate and SO_2

153   As described in Fig. 2, the mass concentrations of $PM_{2.5}$, SO_4^{2-} and SO_2 during the period from 4 to

154   22 Dec. 2019 in NUIST changed from 28.1 to 67.0 μg m^{-3}, 8.3 to 17.8 μg m^{-3} and 6.2 to 20.9 μg m^{-3}

155   with an average and standard deviation at 45.7±12.1 μg m^{-3}, 12.7±3.3 μg m^{-3} and 10.2±4.4 μg m^{-3},

156   respectively. It can be observed that $PM_{2.5}$ average concentration was about 1.3 times of the First Grade

157   National Ambient Air Quality Standard (35 μg m^{-3}) and beyond the safety standard of World Health

158   Organization (10 μg m^{-3}). The photochemical reactivity during the winter in Beijing has been found to

159   be relatively high (Zhang et al., 2020), which facilitates the formation of some photooxidants. The

160   relatively clean days during the sampling period indicates the importance of photoinduced oxidation of
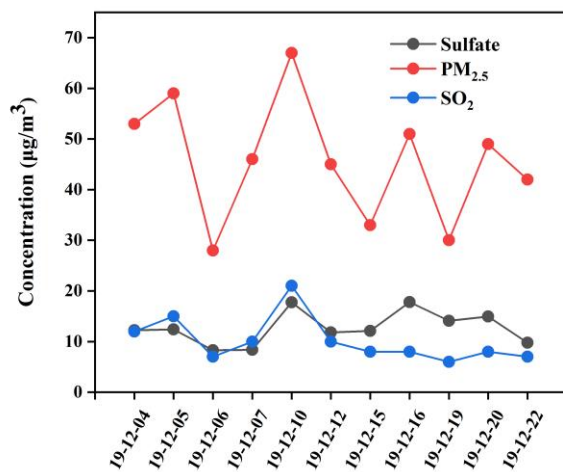
161   SO_2.

163   **Fig. 2.** Variations in concentrations of $PM_{2.5}$, SO_4^{2-} and SO_2.

164   Meanwhile, the change trends of $PM_{2.5}$, SO_4^{2-} and SO_2 concentrations were found to be basically the

165   same during the sampling period, indicating sulfate was mainly from SO_2 oxidation. Especially, $PM_{2.5}$,

166   SO_4^{2-} and SO_2 concentrations increased to the maximum values on 10 Dec.. It is noted that NO_2 and

167   CO concentrations were 85 and 1.60 μg m^{-3} on 10 Dec., which were also the maximum values during

168   the sampling period. Based on the wind speed was lower than 3m s^{-1} and there was presence of static

169 weather during the sampling period, we believed that high CO concentration was mainly from local

170 emissions. However, O_3 concentration on 10 Dec. was the minimum value at 24 $\mu g\ m^{-3}$, which

171 preliminarily indicated that SO_2 oxidation by NO_2 might be a major pathway in sulfate formation.

172 Previous studies showed that SO_2 oxidation by NO_2 in aerosol water dominated heterogeneous sulfate

173 formation during wintertime at neutral aerosol pH (Wang et al., 2016; Cheng et al., 2016). However,

174 subsequent studies showed that the calculated aerosol pH was in the range of 4.2-4.7, and the reactions

175 between SO_2 and NO_2 during this pH range were too slow to produce sulfate. Considering low aerosol

176 pH in Nanjing region, we suggested that SO_2 oxidation by NO_2 was not a dominant pathway for sulfate

177 formation during the sampling period.

178 In contrast, $PM_{2.5}$, SO_4^{2-} and SO_2 concentrations were observed to be at the minimum values on 6

179 Dec.. Similarly, NO_2 and CO concentrations were also at the minimum of 36 and 0.6 $mg\ m^{-3}$,

180 respectively. However, O_3 concentration on 6 Dec. was the maximum at 50 $\mu g\ m^{-3}$. Besides, the rate of

181 SO_2 oxidation with O_3 becomes fast only when pH>5, the reaction rate of SO_2 with O_3 is one hundredth

182 of those with H_2O_2 or TMI when pH<5. Therefore, pH values of actual fine particles at 4-5 in Nanjing

183 region could markedly restrain SO_2 oxidation by O_3. The lowest SO_4^{2-} concentration on 6 Dec. further

184 demonstrated that SO_2 oxidation by O_3 played an insignificant role in sulfate formation.

185 Generally, aqueous-phase oxidation is deemed to be a main process of sulfate formation in

186 atmospheric environment. Shao et al. (2018) believed that heterogeneous sulfate production on aerosols

187 occurred when RH was higher than 50 %. The RH values of the atmosphere ranging from 50.7 to

188 88.9% during the sampling period indicated that sulfate formation was closely related to SO_2

189 heterogeneous oxidation.

190 3.2 Sulfur isotopic compositions in sulfate and SO_2

191 It can be observed from Fig. 3 that the values of $\delta^{34}S-SO_4^{2-}$ were generally higher compared to those

192 of $\delta^{34}S-SO_2$ during the sampling period except that on 16 Dec.. The $\delta^{34}S-SO_4^{2-}$ values ranged from 3.1

193 to 4.7‰ with an average and standard deviation at 4.0±0.6‰, while $\delta^{34}S-SO_2$ values changed from -2.9

194 to 4.7‰ with an average and standard deviation at -0.2±2.3‰. The discrepancy between the values of

195 $\delta^{34}S-SO_4^{2-}$ and $\delta^{34}S-SO_2$ was mainly related to sulfur isotope fractionation effect during SO_2 oxidation

196 to secondary sulfate.

197
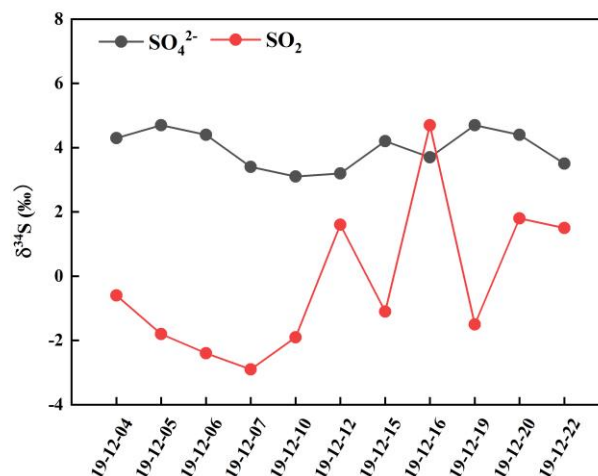
198   **Fig. 3.** Variations in sulfur isotopic compositions in sulfate and SO_2

199   It is noteworthy that $\delta^{34}S$-SO_4^{2-} values were similar to that in $PM_{2.5}$ with an average at 4.2‰ during

200   Youth Olympic Games in Aug. 2014 in Nanjing (Guo et al., 2016). However, the average value of

201      $\delta^{34}S$-SO_4^{2-} during the sampling period was lower than 5.6‰ in Nanjing during a typical haze event

202   from 21 Dec. 2015 to 1 Jan. 2016 (Guo et al., 2019). The higher $\delta^{34}S$ values of sulfate in haze was

203   possibly ascribed to SO_2 heterogeneous oxidation, which typically enriched heavy sulfur isotope in

204   sulfate. In this study, the average concentrations of $PM_{2.5}$ was 45.7 μg m^{-3}, indicating a not heavily

205   polluted time interval. Besides, the relatively high temperature during the sampling period was

206   favorable for photochemical reactions and OH radicals' formation. As a result, the contribution of SO_2

207   homogenous oxidation increased during sulfate formation, which enriched light sulfur isotope

208   compared to that in haze. Han et al. (2017) determined $\delta^{34}S$ values in Beijing $PM_{2.5}$ with an average at

209   6.0‰. It is observed that there existed a regional difference in $\delta^{34}S$-SO_4^{2-} values. The $\delta^{34}S$-SO_4^{2-} value

210   in Nanjing was generally lower than that in Beijing. The discrepancy of $\delta^{34}S$-SO_4^{2-} value illustrated

211   different sulfur sources and SO_2 oxidation pathways in these regions. In addition, $\delta^{34}S$-SO_4^{2-} values

212   presented a seasonal change. $\delta^{34}S$ values in Beijing aerosol sulfate varied from 3.4 to 7.0‰ with an

213   average of 5.0‰ in summer and from 7.1 to 11.3‰ with an average of 8.6‰ in winter. Generally, SO_2

214   homogeneous oxidation dominated in summer compared to that in winter due to strong solar irradiation

215   (Han et al., 2016). SO_2 oxidation might lead to sulfur isotope fractionation, which was mainly

216   attributed to equilibrium or kinetic discrimination between SO_2 and sulfate. The influence of different

217   oxidants on sulfur isotope fractionation needed to be further investigated.

218   Fig.4 presents the relationship between $\delta^{34}S$-SO_4^{2-} value and atmospheric temperature during the

219 sampling period. It can be observed that there existed an obviously negative correlation. The higher

220 temperature generally corresponded to the lower δ^{34}S-SO$_4^{2-}$ value. This is mainly ascribed to kinetic

221 effect of sulfur isotope fractionation during SO$_2$ oxidation. At high temperature, more OH radicals were

222 produced and the contribution of SO$_2$ homogeneous oxidation increased. It is reported that sulfur

223 isotope fractionation about SO$_2$ was -9‰ for homogeneous oxidation process (Tanaka et al., 1994).

224 Therefore, low δ^{34}S value in sulfate at high temperature was chiefly due to the elevated SO$_2$

225 homogeneous oxidation.
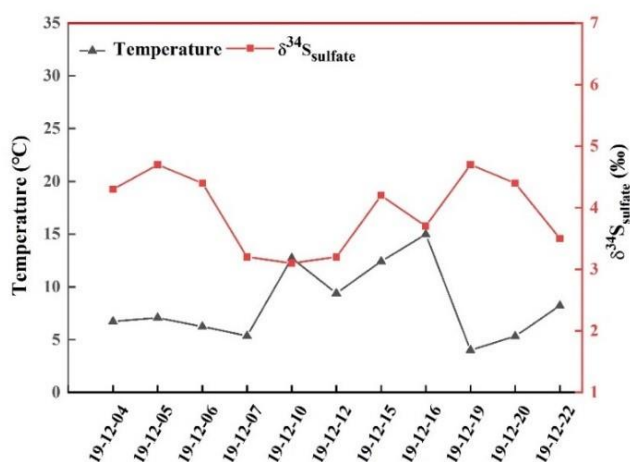
226

227 **Fig. 4.** The correlation between δ^{34}S-SO$_4^{2-}$ value and atmospheric temperature.

228 3.3 Sulfur isotope fractionation during SO$_2$ oxidation

229 The secondary sulfate was generally from SO$_2$ homogeneous and heterogeneous oxidation (Seinfeld

230 and Pandis, 1998). The homogeneous and heterogeneous oxidation of SO$_2$ might lead to sulfur isotope

231 fractionation, which is described by using fractionation coefficient (α)

$$\alpha=\frac{\dfrac{\delta^{34}S_{SO_4^{2-}}}{10^3}+1}{\dfrac{\delta^{34}S_{SO_2}}{10^3}+1} \tag{1}$$

232

233 Sulfate enriched heavy sulfur isotope (α>1) during SO$_2$ heterogeneous oxidation for the presence of

234 isotope equilibrium fractionation and kinetic fractionation. However, sulfate enriched light sulfur

235 isotope (α<1) during SO$_2$ homogeneous oxidation due to this process was only related to kinetic

236 fractionation. As described in Fig. 5, α values ranged from 0.9988 to 1.0201 indicating there existed

237 SO$_2$ homogeneous and heterogeneous oxidation during the sampling period. α value was at the

238 minimum of 0.9988 on 16 Dec., which showed SO$_2$ homogeneous oxidation played a crucial role.
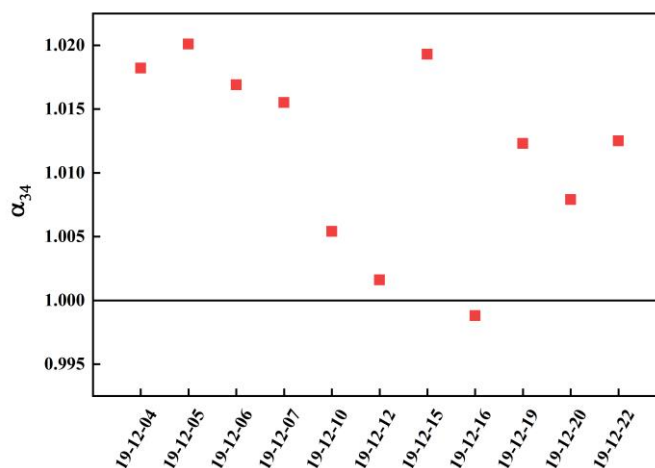
Fig. 5. Sulfur isotope fractionation coefficients during SO_2 oxidation.

It is reported that sulfur isotope fractionations during SO_2 heterogeneous and homogeneous oxidation to sulfate were 16.5‰ and -9‰, respectively (Tanaka et al., 1994). Consequently, the contribution of SO_2 heterogeneous and homogeneous oxidation to sulfate could be calculated by sulfur isotope mass equilibrium equations (2) and (3).

$$\delta^{34}S_{SO_2}+16.5x-9y=\delta^{34}S_{SO_4^{2-}} \tag{2}$$

$$x+y=1 \tag{3}$$

where x and y represent the contribution of SO_2 heterogeneous and homogeneous oxidation, respectively.

It is observed from Fig. 6 that most of the days (7 out of 11) had more than 50% contributions from SO_2 heterogeneous oxidation, which indicated that SO_2 heterogeneous oxidation was generally dominant during sulfate formation. He et al. (2018) presented the observations of oxygen-17 excess of $PM_{2.5}$ sulfate collected in Beijing haze from Oct. 2014 to Jan. 2015, and found the contribution of heterogeneous sulfate production was about 41-54% with a mean of 48±5%. The contribution of SO_2 heterogeneous oxidation reached high-level during 5-7 Dec. and on 19 Dec., which was closely related to the temperature of the atmosphere. The low temperature about 5 ℃ during these days was favorable for SO_2 dissolution in water and further oxidized to sulfate. On 16 Dec., the contribution of SO_2 heterogeneous oxidation was at the minimum of 31.4%. The highest temperature of 15 ℃ on 16 Dec. restrained SO_2 solubility in aqueous solution and facilitated to produce lots of gaseous oxidants such as OH radicals to promote SO_2 homogeneous oxidation.

260
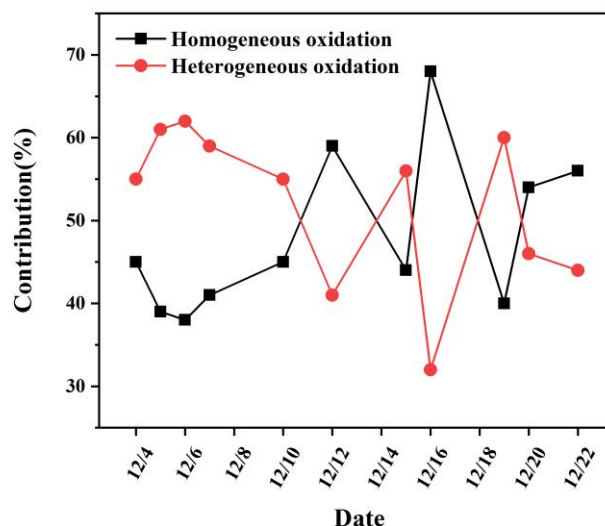
261   **Fig. 6.** The contributions of SO_2 heterogeneous and homogeneous oxidation to sulfate.

262   Overall, the temperature was an important factor in controlling SO_2 oxidation pathways. High

263 temperature facilitated kinetic fractionation of sulfur isotope during SO_2 oxidation to sulfate, thereby

264 decreasing $\delta^{34}S$ value in sulfate. In addition, there was lack of positive correlation between the

265 contribution of SO_2 heterogeneous oxidation and O_3 or NO_2 concentration. This further demonstrated

266 that SO_2 oxidation by O_3 and NO_2 were not the important pathways during the sampling period.

267 Consequently, we mainly focused on SO_2 heterogeneous oxidation by H_2O_2 and Fe^{3+}/O_2 in the

268 following study.

269 3.4 The correlation of $\delta^{18}O$ values between H_2O and SO_4^{2-} from SO_2 oxidation by H_2O_2 and Fe^{3+}/O_2

270   It is known that SO_2 rapidly equilibrates with ambient water for very high molar ratio of H_2O to SO_2

271 in the atmosphere. As a result, $\delta^{18}O$ value of SO_2 is dynamically controlled by $\delta^{18}O$ value of water and

272 $\delta^{18}O$ value of SO_2 has no obvious effect on $\delta^{18}O$ value of sulfate produced from different oxidation

273 pathways. Meanwhile, sulfate is very stable with respect to O atom exchange with ambient water.

274 Consequently, $\delta^{18}O$ can be adopted to distinguish SO_2 oxidation processes due to that $\delta^{18}O$ value of

275 product sulfate reflected the distinctive signals of different oxidants.

276   We simulatively studied SO_2 heterogeneous oxidation by H_2O_2 and Fe^{3+}/O_2 in the laboratory, which

277 aims to make clear the relationship of $\delta^{18}O$ values between product sulfate and three kinds of water at

278 10 ℃. It can be observed from Fig. 7 that $\delta^{18}O$ value of sulfate was linearly dependent on $\delta^{18}O$ value of

279 water, and the slope of linear curve for H_2O_2 oxidation approximates a ratio of 0.43, indicating that the

280 isotopy of about two of four oxygen atoms in sulfate was controlled by $\delta^{18}O$ value of water. The other

281 two oxygen atoms were from H_2O_2 molecules, whose O-O bond remained intact during SO_2 oxidation.

282 In addition, we noted from Fig. 7 that the slope of linear curve for Fe^{3+}/O_2 oxidation was about 0.65,

283 which represented that the isotopy of about three of four oxygen atoms in sulfate was related to $\delta^{18}O$

284 value of water. A 3/4 control of sulfate oxygens by water is also characteristic of heterogeneous

285 oxidation mechanisms in which HSO_3^- isotopically equilibrated with water prior to significant

286 oxidation to SO_4^{2-}. The other one oxygen atom in sulfate was from O_2. The higher slope suggested a

287 higher dependence of $\delta^{18}O$ value of sulfate on $\delta^{18}O$ value of water during SO_2 heterogeneous oxidation

288 by Fe^{3+}/O_2. The discrepancy of the slopes for different SO_2 heterogeneous oxidation processes provides

289 us a potential method to distinguish SO_2 oxidation pathways.
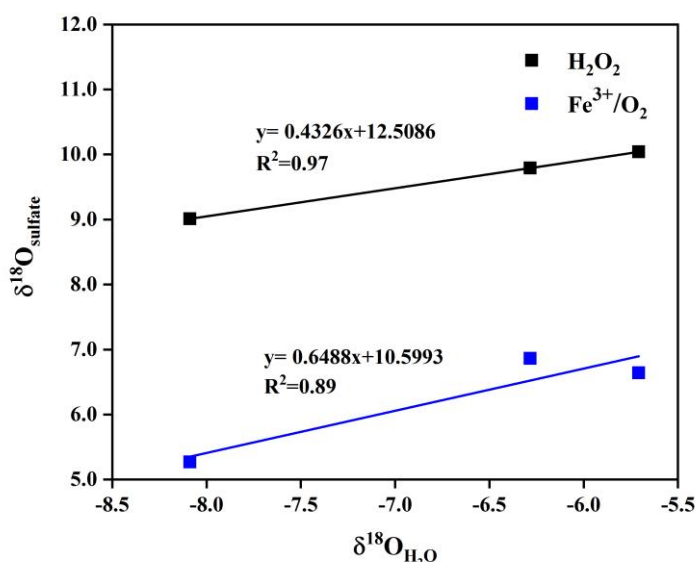
290

291 **Fig.7.** The correlation of $\delta^{18}O$ values between H_2O and sulfate from SO_2 oxidation by H_2O_2 and

292 Fe^{3+}/O_2, respectively.

293 3.5 $\delta^{18}O$-SO_4^{2-} values in $PM_{2.5}$ and SO_2 main oxidation pathways

294 As depicted in Fig. 8, $\delta^{18}O$ values of sulfate in $PM_{2.5}$ ranged from 11.09 to 12.93‰ with an average

295 and standard deviation of 12.35±0.68‰. $\delta^{18}O$ values of sulfate focused on a narrow scope except those

296 on 5 and 22 Dec.. It should be pointed out $\delta^{18}O$ value of secondary sulfate was a comprehensive result

297 from different SO_2 oxidation processes. Sulfate in $PM_{2.5}$ usually consisted of primary sulfate and

298 secondary sulfate. The $\delta^{18}O$ value of primary sulfate is about 38‰ (Holt and Kumar, 1984), which is

299 significantly higher than those of secondary sulfate. The contribution of primary and secondary sulfate

300
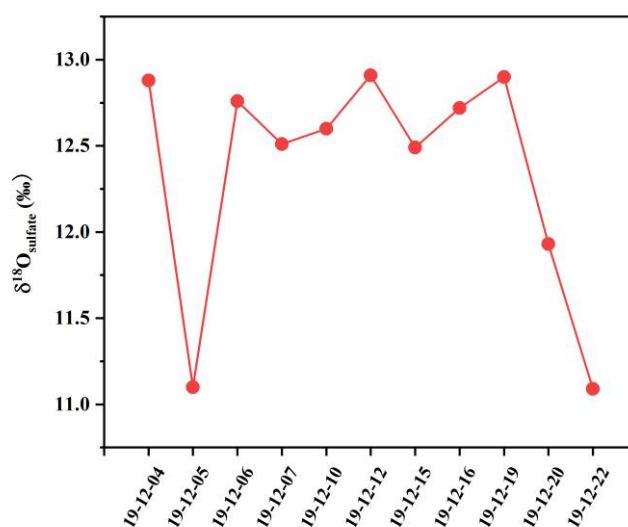
301   **Fig.8.** $\delta^{18}O$ values of sulfate in $PM_{2.5}$ during the sampling period.

302   in the atmosphere can be calculated by oxygen isotope mass equilibrium equation (4) (Ben et al.,

303   1982).

304    $$\delta^{18}O_{PM_{2.5}}=\delta^{18}O_{PS}\times (1-f_{SS}) + \delta^{18}O_{SS}\times f_{SS}$$ (4)

305   where $\delta^{18}O_{PM_{2.5}}$, $\delta^{18}O_{PS}$ and $\delta^{18}O_{SS}$ mean $\delta^{18}O$ values of $PM_{2.5}$, primary sulfate and secondary sulfate,

306   respectively; f_{SS} is the contribution of secondary sulfate in $PM_{2.5}$.

307   It is noteworthy from Fig. 9 that there exists a linear relationship between $\delta^{18}O$ values in water and

308   secondary sulfate from different SO_2 oxidation pathways, and this can be described by the equations

309   (5)-(7), where the value of $\delta^{18}O_{water}$ is about -6.2‰ in Nanjing region. As discussed above, secondary

310   sulfate was mainly ascribed to SO_2 homogeneous oxidation by OH radicals and heterogeneous

311   oxidation by H_2O_2 and Fe^{3+}/O_2. Therefore, $\delta^{18}O_{SS}$ value in equation (4) can be obtained based on

312   equations (5)-(7), respectively. As a result, the average contribution of primary and secondary sulfate in

313    $PM_{2.5}$ are presented in Table 1. It can be observed that the majority of sulfate in $PM_{2.5}$ was secondary

314   sulfate, which appears to constitute from 79.9 to 86.2% of total sulfate during the sampling period. It is

315   admirable to quantitively describe these formation pathways of secondary sulfate in $PM_{2.5}$.

316    $$\delta^{18}O_{SS}=0.69\times\delta^{18}O_{water}+9.5\ ‰\ (OH)\ (Holt\ and\ Kumar,\ 1984)$$ (5)

317    $$\delta^{18}O_{SS}=0.65\times\delta^{18}O_{water}+10.6\ ‰\ (Fe^{3+}/O_2)\ (this\ study)$$ (6)

318    $$\delta^{18}O_{SS}=0.43\times\delta^{18}O_{water}+12.5\ ‰\ (H_2O_2)\ (this\ study)$$ (7)

319
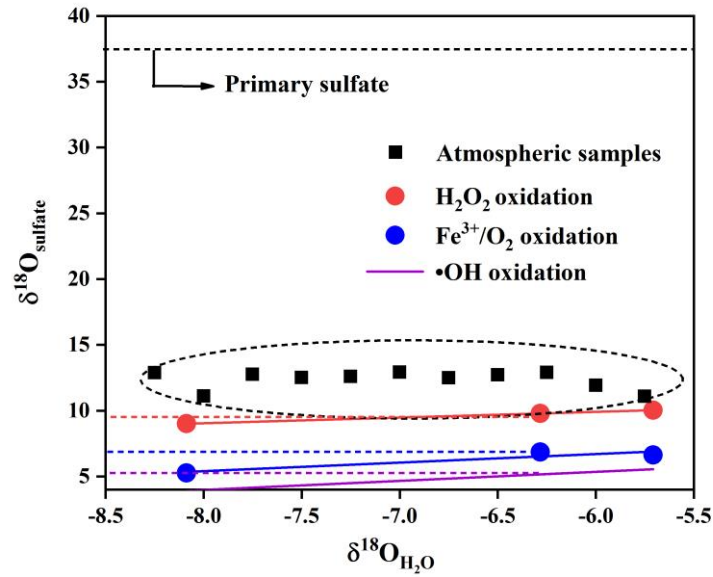
Fig.9. The correlation between δ¹⁸O values in water and sulfate in PM$_{2.5}$.

321

Table 1 The average contribution of primary sulfate and secondary sulfate in PM$_{2.5}$.

Sampling time	Primary sulfate (%)	Secondary sulfate (%)
4 Dec.	19.7	80.3
5 Dec.	13.9	86.1
6 Dec.	19.3	80.7
7 Dec.	18.4	81.6
10 Dec.	18.7	81.3
12 Dec.	20.0	80.0
15 Dec.	18.4	81.6
16 Dec.	20.1	79.9
19 Dec.	19.7	80.3
20 Dec.	16.7	83.3
22 Dec.	13.8	86.2

322

323   According to the percentages of SO$_2$ heterogeneous and homogeneous oxidation to sulfate in Fig.6

324 and the average contributions of primary sulfate and secondary sulfate in PM$_{2.5}$ in Table 1, we can

325 further calculate the ratios of different SO$_2$ oxidation pathways at 10 ℃ via oxygen isotope mass

326 equilibrium equations (8)-(10), and the corresponding results are depicted in Table 2.

$$\delta^{18}O_{PM_{2.5}}=\delta^{18}O_{PS}\times f_{PS}+ (\delta^{18}O_{SS\text{-}OH}\times f_{SS\text{-}OH}+\delta^{18}O_{SS\text{-}Fe^{3+}/O_2}\times f_{SS\text{-}Fe^{3+}/O_2}+\delta^{18}O_{SS\text{-}H_2O_2}\times f_{SS\text{-}H_2O_2})\times f_{SS} \tag{8}$$

$$f_{PS}+f_{SS}=1 \tag{9}$$

$$f_{SS\text{-}OH}+f_{SS\text{-}Fe^{3+}/O_2}+f_{SS\text{-}H_2O_2}=1 \tag{10}$$

where $\delta^{18}O_{PM_{2.5}}$ and $\delta^{18}O_{PS}$ are $\delta^{18}O$ values of total sulfate and primary sulfate in $PM_{2.5}$; $\delta^{18}O_{SS\text{-}OH}$, $\delta^{18}O_{SS\text{-}Fe^{3+}/O_2}$ and $\delta^{18}O_{SS\text{-}H_2O_2}$ are $\delta^{18}O$ values of secondary sulfate from SO_2 oxidation by OH radicals, Fe^{3+}/O_2 and H_2O_2, respectively; f_{PS} and f_{SS} are the contribution of primary and secondary sulfate; $f_{SS\text{-}OH}$, $f_{SS\text{-}Fe^{3+}/O_2}$ and $f_{SS\text{-}H_2O_2}$ are the ratios of secondary sulfate from SO_2 oxidation by OH radicals, Fe^{3+}/O_2 and H_2O_2, respectively.

Unlike heavily polluted days with reduced solar irradiation, the photochemical reactivity can remain high in clean days during the observation period because of relatively intense solar irradiation. As a result, some photochemical reactive species such as OH radicals and H_2O_2 are deemed to be the major oxidants for sulfate formation. Generally, H_2O_2 production in the relatively clean atmosphere is ascribed to self-reaction of HO_2 radicals that mainly come from the reactions of OH radicals with CO and volatile organic compounds. It is observed from Table 2 that the ratios of SO_2 oxidation by OH radicals ranged from 38 to 68% with an average and standard deviation at 48±9.7%. The ratio reached the maximum of 68% on 16 Dec., which is mainly ascribed to the highest temperature of 15 °C during the sampling period. The photochemical reactions are favorable for producing more OH radicals. In contrast, the ratio of SO_2 oxidation by OH radicals decreased to the minimum of 38% on 6 Dec. due to the low temperature.

Table 2 The ratios of SO_2 different oxidation pathways to sulfate.

Time	$f_{SS\text{-}OH}$	$f_{SS\text{-}H_2O_2}$	$f_{SS\text{-}Fe^{3+}/O_2}$	$f_{SS\text{-}H_2O_2}/(f_{SS\text{-}H_2O_2}+f_{SS\text{-}Fe^{3+}/O_2}$ (%)
4 Dec.	0.45	0.27	0.28	49.1
5 Dec.	0.39	0.24	0.37	39.3
6 Dec.	0.38	0.24	0.38	38.7
7 Dec.	0.41	0.25	0.34	42.3
10 Dec.	0.45	0.27	0.28	49.1
12 Dec.	0.59	0.30	0.11	73.2
15 Dec.	0.44	0.26	0.30	46.5
16 Dec.	0.68	0.26	0.06	81.2

19 Dec.	0.40	0.25	0.35	41.6
20 Dec.	0.54	0.31	0.15	67.4
22 Dec.	0.56	0.32	0.12	72.7

It is known that SO_2 oxidation by H_2O_2 and Fe^{3+}/O_2 are the most important pathways during SO_2 heterogeneous oxidation. It can be observed from table 2 that the percentage of sulfate from SO_2 oxidation by H_2O_2 in secondary sulfate from SO_2 heterogeneous oxidation changed from 38.7 to 81.2% with an average and standard deviation at 54.6±15.7%, indicating that SO_2 oxidation by H_2O_2 predominated during SO_2 heterogeneous oxidation. In addition, there existed an obviously positive correlation between the ratios of SO_2 oxidation by H_2O_2 and OH radicals, which was chiefly attributed to the photochemical reactions. The relatively strong solar irradiation on 16 Dec. resulted in the maximum ratio of 81.2% about H_2O_2 oxidation in SO_2 heterogeneous reactions. The sampling site is close to Nanjing steel plant. As companion emitters, Fe^{3+} are present in much higher concentrations than that in other areas. It is believed that SO_2 oxidation by O_2 in the presence of Fe^{3+} was not negligent in the areas where the concentrations of SO_2 and Fe^{3+} were high. This inevitably resulted in high SO_2 oxidation ratio by Fe^{3+}/O_2 in SO_2 heterogeneous oxidation processes.

4 Conclusions

There was no serious $PM_{2.5}$ pollution during the sampling period. The secondary sulfate constitutes from 79.9 to 86.2% of total sulfate in $PM_{2.5}$. SO_2 oxidation by O_3 and NO_2 played an insignificant role in sulfate formation. The secondary sulfate was mainly ascribed to SO_2 homogeneous oxidation by OH radicals and heterogeneous oxidation by H_2O_2 and Fe^{3+}/O_2. Compared to homogeneous oxidation, SO_2 heterogeneous oxidation was generally dominant with an average contribution of 51.6%. SO_2 oxidation by H_2O_2 predominated in SO_2 heterogeneous oxidation reactions and the average ratio of which reached 54.6%. Consequently, sulfur and oxygen isotopes can be used to gain an insight into sulfate formation. The determination of sulfur isotopic compositions in SO_2 and sulfate are advantageous to quantify the contribution of SO_2 homogeneous and heterogeneous oxidation. Combining field observations of oxygen isotope in the atmosphere with the linear relationships of $\delta^{18}O$ values between H_2O and sulfate from different SO_2 oxidation processes can obtain an increased understanding of specific sulfate formation pathways. This study is favorable for deeply investigating sulfur cycle in the

atmosphere.

Author contribution

Ziyan Guo carried out the experiment and wrote the original draft. Keding Lu designed the methodology and administrated the project. Pengxiang Qiu and Mingyi Xu performed the data collection. Zhaobing Guo instructed the experiment and revised the paper.

Competing interests

The authors declare that they have no competing interest that can influence the work reported in this paper.

Acknowledgement

We gratefully acknowledge the financial supports from the National Natural Science Foundation of China (Nos. 41873016, 51908294, and 21976006), the National Science Fund for Distinguished Young Scholars (No. 22325601).

References

Abbatt, J. P. D., Benz, S., Cziczo, D. J., Kanji, Z., Lohmann, U., and Mohler, O.: Solid ammonium sulfate aerosols as ice nuclei: a pathway for cirrus cloud formation, Science, 313, 1770-1773, https://doi.org/10.1126/science.1129726, 2006.

Ben, D. H., Romesh, K., and Paul, T. C.: Primary Sulfates in Atmospheric Sulfates: Estimation by Oxygen Isotope Ratio Measurements, Science, 217, 51-53, https://doi.org/10.1126/science.217.4554.51, 1982.

Brüggemann, M., Riva, M., Perrier, S., Poulain, L., George, C., and Herrmann, H.: Overestimation of Monoterpene Organosulfate Abundance in Aerosol Particles by Sampling in the Presence of SO_2, Environ. Sci. Technol. Lett., 8, 206-211, https://doi.org/10.1021/acs.estlett.0c00814, 2021.

Cheng, Y. F., Zheng, G. J., Wei, C., Mu, Q., Zheng, B., Wang, Z. B., Gao, M., Zhang, Q., He, K. B., Carmichael, G., Pöschl, U., and Su, H.: Reactive Nitrogen Chemistry in Aerosol Water as a Source of Sulfate during Haze Events in China, Sci. Adv., 2, e1601530, https://doi.org/10.1126/sciadv.1601530, 2016.

Gao, J., Wei, Y., Zhao, H., Liang, D., Feng, Y., and Shi, G.: The role of source emissions in sulfate formation pathways based on chemical thermodynamics and kinetics model, Sci. Total. Environ., 851, 158104, https://doi.org/10.1016/j.scitotenv.2022.158104, 2022.

Guo, Z. B., Shi, L., Chen, S. L., Jiang, W. J., Wei, Y., Rui, M. L., and Zeng, G.: Sulfur isotopic fractionation and source apportionment of $PM_{2.5}$ in Nanjing region around the second session of the Youth Olympic Games, Atmos. Res., 174-175, 9-17, https://doi.org/10.1016/j.atmosres.2016.01.011, 2016.

Guo, Z. Y., Guo, Q. J., Chen, S. L., Zhu, B., Zhang, Y., Yu, J., and Guo, Z. B.: Study on pollution behavior and sulfate formation during the typical haze event in Nanjing with water soluble inorganic ions and sulfur isotopes, Atmos. Res., 217, 198-207, https://doi.org/10.1016/j.atmosres.2018.11.009, 2019.

Han, X. K., Guo, Q. J., Liu, C. Q., Fu, P. Q., Strauss, H., Yang, J., Jian, H., Wei, L., Hong, R., Peters, M., Wei, R. F., and Tian, L.: Using stable isotopes to trace sources and formation processes of sulfate aerosols from Beijing, China, Sci. Rep., 6, 29958, https://doi.org/10.1038/srep29958, 2016.

Han, X. K., Guo, Q. J., Strauss, H., Liu, C. Q., Hu, J., Guo, Z. B., Wei, R. F., Peters, M., Tian, L., and

417 Kong, J.: Multiple Sulfur Isotope Constraints on Sources and Formation Processes of Sulfate in Beijing

418 $PM_{2.5}$ Aerosol, Environ. Sci. Technol., 51, 7794-7803, https://doi.org/10.1021/acs.est.7b00280, 2017.

419 Harris, E., Sinha, B., Hoppe, P., and Ono, S.: High-precision measurements of ^{33}S and ^{34}S fractionation

420 during SO_2 oxidation reveal causes of seasonality in SO_2 and sulfate isotopic composition, Environ. Sci.

421 Technol., 47, 12174-12183, https://doi.org/10.1021/es402824c, 2013.

422 Harris, E., Sinha, B., Hoppe, P., Crowley, J. N., Ono, S., and Foley, S.: Sulfur isotope fractionation

423 during oxidation of sulfur dioxide: gas-phase oxidation by OH radicals and aqueous oxidation by H_2O_2,

424 O_3 and iron catalysis, Atmos. Chem. Phys., 12, 407-424, https://doi.org/10.5194/acp-12-407-2012,

425 2012.

426 He, P. Z., Alexander, B., Geng, L., Chi, X. Y., Fan, S. D., Zhan, H. C., Kang, H., Zheng, G. J., Cheng, Y.

427 F., Su, H., Liu, C., and Xie, Z. Q.: Isotopic constraints on heterogeneous sulfate production in Beijing

428 haze, Atmos. Chem. Phys., 18, 5515-5528, https://doi.org/10.5194/acp-18-5515-2018, 2018.

429 He, X., Wu, J. J., Ma, Z. C., Xi, X., and Zhang, Y. H.: NH_3-promoted heterogeneous reaction of SO_2 to

430 sulfate on α-Fe_2O_3 particles with coexistence of NO_2 under different relative humidities, Atmos.

431 Environ., 262, 118622, https://doi.org/10.1016/j.atmosenv.2021.118622, 2021.

432 Holt, B.D. and Kumar R.: Oxygen-18 study of high-temperature air oxidation of SO_2, Atmos. Environ.,

433 18, 2089-2094, https://doi.org/10.1016/0004-6981(84)90194-X, 1984.

434 Huang, R. J., Zhang, Y., Bozzetti, C., Ho, K. F., Cao, J. J., Han,Y., Daellenbach, K. R., Slowik, J. G.,

435 Platt, S. M., Canonaco, F., Zotter, P., Wolf, R., Pieber, S. M., Bruns, E. A., Crippa, M., Ciarelli, G.,

436 Piazzalunga, A., Schwikowski, M., Abbaszade, G., Schnelle-Kreis, J., Zimmermann, R., An, Z., Szidat,

437 S., Baltensperger, U., El Haddad, I., and Prevot, A. S.: High secondary aerosol contribution to

438 particulate   pollution   during   haze   events   in   China,   Nature,   514,   218-222,

439 https://doi.org/10.1038/nature13774, 2014.

440 Kuang, B., Zhang, F., Shen, J., Shen, Y., Qu, F., Jin, L., Tang, Q., Tian, X., and Wang, Z.: Chemical

441 characterization, formation mechanisms and source apportionment of $PM_{2.5}$ in north Zhejiang Province:

442 The importance of secondary formation and vehicle emission, Sci. Total. Environ., 851, 158206,

443 https://doi.org/10.1016/j.scitotenv.2022.158206, 2022.

444 Li, J. H. Y., Zhang, Y. L., Cao, F., Zhang, W., and Michalski, G.: Stable Sulfur Isotopes Revealed a

445 Major Role of Transition-Metal Ion-Catalyzed SO_2 Oxidation in Haze Episodes, Environ. Sci. Technol.,

54, 2626-2634, https://doi.org/10.1021/acs.est.9b07150, 2020.

Lin, Y. C., Yu, M., Xie, F., and Zhang, Y.: Anthropogenic Emission Sources of Sulfate Aerosols in Hangzhou, East China: Insights from Isotope Techniques with Consideration of Fractionation Effects between Gas-to-Particle Transformations, Environ. Sci. Technol., 56, 3905-3914. https://doi.org/110.1021/acs.est.1c05823, 2022.

Liu, M. X., Song, Y., Zhou, T., Xu, Z. Y., Yan, C. Q., Zheng, M., Wu, Z. J., Hu, M., Wu, Y. S., and Zhu, T.: Fine particle pH during severe haze episodes in northern China, Geophys. Res. Lett., 44, 5213-5221, https://doi.org/10.1002/2017GL073210, 2017.

Liu, T., Clegg, S. L., Abbatt, J. P. D.: Fast oxidation of sulfur dioxide by hydrogen peroxide in deliquesced aerosol particles, Proc. Natl Acad. Sci. USA., 117, 1354-1359, https://doi.org/10.1073/pnas.1916401117, 2020.

Liu, Y. Y., Wang, T., Fang, X. Z., Deng, Y., Cheng, H. Y., Nabi, I., and Zhang, L.: Brown carbon: An underlying driving force for rapid atmospheric sulfate formation and haze event, Sci. Total. Environ., 734, 139415, https://doi.org/10.1016/j.scitotenv.2020.139415, 2020.

Meng, X., Hang, Y., Lin, X., Li, T. T., Wang, T. J., Cao, J. J., Fu, Q. Y., Dey, S., Huang, K., Liang, F. C., Kan, H. D., Shi, X. M., and Liu, Y.: A satellite-driven model to estimate long-term particulate sulfate levels and attributable mortality burden in China, Environ. Int., 171,107740, https://doi.org/10.1016/j.envint.2023.107740, 2023.

Oh, S. H., Park, K., Park, M., Song, M., Jang, K. S., Schauer, J. J., Bae, G. N., and Bae, M. S.: Comparison of the sources and oxidative potential of $PM_{2.5}$ during winter time in large cities in China and South Korea, Sci. Total. Environ., 859, 160369, https://doi.org/10.1016/j.scitotenv.2022.160369, 2023.

Ramanathan, V., Crutzen, P. J., Kiehl, J. T., and Rosenfeld, D.: Aerosols, climate, and the hydrological cycle, Science, 294, 2119-2124, https://doi.org/10.1126/science.1064034, 2001.

Seinfeld, J. H. and Pandis, S. N.: Atmospheric Chemistry and Physics: From Air Pollution to Climate Change, Phys. Today, 51, 88-90, https://doi.org/10.1063/1.882420, 1998.

Shao, J. Y., Chen, Q. J., Wang, Y. X., Lu, X., He, P. Z., Sun, Y. L., Shah, V., Martin, R. V., Philip, S., Song, S. J., Zhao, Y., Xie, Z. Q., Zhang, L., and Alexander, B.: Heterogeneous sulfate aerosol formation mechanisms during wintertime Chinese haze events: air quality model assessment using observations

of sulfate oxygen isotopes in Beijing, Atmos. Chem. Phys., 19, 6107-6123, https://doi.org/10.5194/acp-19-6107-2019, 2019.

Tanaka, N., Rye, D. M., Xiao, Y., and Lassaga, A. C.: Use of stable sulfur isotope systematic for evaluating oxidation reaction pathways and in-cloud scavenging of sulfur dioxide in the atmosphere, Geophys. Res. Lett., 21, 1519-1522, https://doi.org/10.1029/94GL00893, 1994.

Wang, G. H., Zhang, R. Y., Gomez, M. E., Yang, L. X., Levy Zamora, M., Hu, M., Lin, Y., Peng, J. F., Guo, S., Meng, J. J., Li, J. J., Cheng, C. L., Hu, T. F., Ren, Y. Q., Wang, Y. S., Gao, J., Cao, J. J., An, Z. S., Zhou, W. J., Li, G. H., Wang, J. Y., Tian, P. F., Marrero-Ortiz, W., Secrest, J., Du, Z. F., Zheng, J., Shang, D. J., Zeng, L. M., Shao, M., Wang, W. G., Huang, Y., Wang, Y., Zhu, Y. J., Li, Y. X., Hu, J. X., Pan, B., Cai, L., Cheng, Y. T., Ji, Y. M., Zhang, F., Rosenfeld, D., Liss, P. S., Duce, R. A., Kolb, C. E., and Molina, M. J.: Persistent sulfate formation from London Fog to Chinese haze, Proc. Natl. Acad. Sci. U.S.A., 113, 13630-13635, https://doi.org/10.1073/pnas.1616540113, 2016.

Wang, W. G., Liu, M. Y., Wang, T. T., Song, Y., Zhou, L., Cao, J. J., Zhu, T., Tian, H. Z., and Ge, M. F.: Sulfate formation is dominated by manganese-catalyzed oxidation of SO_2 on aerosol surfaces during haze events, Nat. Commun., 12, 1993, https://doi.org/10.1038/s41467-021-22091-6, 2021.

Xue, J., Yuan, Z., Griffith, S. M., Yu, X., Lau, A. K. H., and Yu, J. Z.: Sulfate Formation Enhanced by a Cocktail of High NO_x, SO_2, Particulate Matter, and Droplet pH during Haze-Fog Events in Megacities in China: An Observation-Based Modeling Investigation, Environ. Sci. Technol., 50, 7325-7334, https://doi.org/10.1021/acs.est.6b00768, 2016.

Xue, J., Yuan, Z., Yu, J. Z., and Lau, A. K. H.: An Observation-Based Model for Secondary Inorganic Aerosols, Aerosol Air Qual. Res., 14, 862-878, https://doi.org/10.4209/aaqr.2013.06.0188, 2014.

Yang, T., Xu, Y., Ye, Q., Ma, Y. J., Wang, Y. C., Yu, J. Z., Duan, Y. S., Li, C. X., Xiao, H. W., Li, Z. Y., Zhao, Y., and Xiao, H. Y.: Spatial and diurnal variations of aerosol organosulfates in summertime Shanghai, China: potential influence of photochemical processes and anthropogenic sulfate pollution, Atmos. Chem. Phys., 23, 13433-13450, https://doi.org/10.5194/acp-23-13433-2023, 2023.

Ye, C., Liu, P. F., Ma, Z. B., Xue, C. Y., Zhang, C. L., Zhang, Y. Y., Liu, J. F., Liu, C. T., Sun, X., and Mu, Y. J.: High H_2O_2 Concentrations Observed during Haze Periods during the Winter in Beijing: Importance of H_2O_2 Oxidation in Sulfate Formation, Environ. Sci. Technol. Lett., 5, 757-763, https://doi.org/10.1021/acs.estlett.8b00579, 2018.

504   Zhang, R., Sun, X. S., Shi, A. J., Huang, Y. H., Yan, J., Nie, T., Yan, X., and Li, X.: Secondary

505   inorganic aerosols formation during haze episodes at an urban site in Beijing, China, Atmos. Environ.,

506   177, 275-282, https://doi.org/10.1016/j.jes.2022.01.008, 2018.

507   Zhang, Y., Bao, F. X., Li, M., Xia, H. L., Huang, D., Chen C. C., and Zhao, J. C.: Photoinduced Uptake

508   and Oxidation of SO_2 on Beijing Urban $PM_{2.5}$, Environ. Sci. Technol., 54,

509   14868-14876, https://doi.org/10.1021/acs.est.0c01532, 2020.